Evaluation and Visualization of Stress and Strain on Soft Biological Tissues in Contact

Sofiane Sarni, Anderson Maciel, Ronan Boulic, Daniel Thalmann
Virtual Reality Lab (VRlab), Swiss Federal Institute of Technology (EPFL)
CH-1015 Lausanne, Switzerland.
sofiane.sarni@epfl.ch, anderson.maciel@epfl.ch, ronan.boulic@epfl.ch, daniel.thalmann@epfl.ch

Abstract

This paper addresses evaluation and visualization of stress and strain on soft biological tissues in contact. Given three-dimensional models of reconstructed organs from magnetic resonance images (MRI), we use an Anatomy-based kinematical model combined with a soft tissues model to represent their shape and behavior. Then, we compute resulting distribution of stress and strain on deforming surface when motion is simulated. The computed stress and strain are then effectively visualized using an interactive animation framework. Experimental results are illustrated in the case of the hip joint cartilage.

1. Introduction

Evaluation of stress and strain is a typical analysis method of three-dimensional bodies. It allows estimating the deformation of an object under given load conditions. That is why it is being widely used in CAD/CAM applications and also in medical applications, especially those related to biomechanics where it is important to assess joints congruity [6]. For instance, assessing stress and strain allows analyzing joint surface, which helps in diagnosing possible pathologies or planning surgery.

Approaches for modeling object deformation range from non-physical methods to methods based on continuum mechanics which account for the effects of material properties, external forces, and environmental constraints or object deformation [9]. Here we focus on specific physically based approaches, which are used for modeling soft tissues and compute related physical quantities. In this category, we find mass-spring systems and finite element methods. Other physically based methods used to model deformable objects include implicit surfaces and particles systems but are not considered here.

Our approach to model soft tissues relies on a generalized mass-spring model where mass points are, in fact, spherical mass regions called molecules. Elastic forces are established between molecules by spring-like connections. This model integrates properties of real biological materials to define the stiffness of those connections.

We compute the distribution of stress and strain on deforming surface when motion is simulated. The stress and strain calculated by means of the deformation model are color mapped on the meshes representing organs to indicate variation during motion. Experimental results are illustrated in the case of hip joint cartilage.

2. Related Work

2.1. Mass-spring systems

The mass-spring method is a physically based technique that has been used widely and effectively for modeling deformable objects. An object is modeled as a collection of point masses connected by springs in a lattice structure. Springs connecting point masses exert forces on neighboring points when a mass is displaced from its rest position (Figure 1).

Mass-spring systems have been widely used in facial animation. Terzopoulos and Waters used a three-layers mesh of mass points associated to three anatomically distinct layers of facial tissue (dermis, subcutaneous fatty tissue, and muscle) [23]. To improve realism, Lee et al. added further constraints to prevent penetrations between soft tissues and bone [13]. In [20], mass-spring systems were used to simulate muscle deformation. Muscles were represented at two levels: action lines and muscle shape. This shape was deformed using a mass-spring mesh. In order to control the volume of muscles during deformation and smooth out mesh discontinuities, “angular springs” were introduced. These springs differ from other springs by the way they are attached. In this work, emphasis was put on interaction rather than simulation quality. Aubel used a similar approach with a multi-layered model based on physiological and anatomical considerations [1]. Bourguignon and Cani proposed a model offering control of the isotropy or anisotropy of elastic material [3]. Mass-spring models do not have this property. The basic idea of their approach is to let the user define, everywhere in the object, mechanical characteristics of the material along a

given number of axes corresponding to orientation of interest. All internal forces will be acting along these axes instead of acting along the mesh edges. Mass spring systems have also been used for cloth motion [2] and surgical simulation [21][5]. In a more recent work, Jansson et al. used a discrete mechanical model that can be viewed as a generalized mass-spring model for applications in computer-aided design [11].

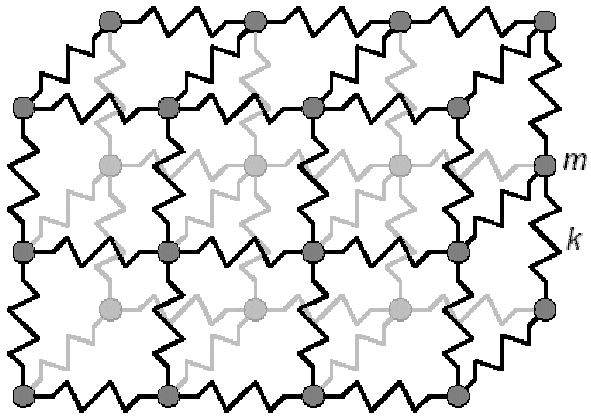

Figure 1. Portion of a mass-spring model. (Reprinted from [9])

Mass-spring models are easy to construct, and both interactive and real-time simulations of mass-spring systems are possible even with desktop systems. Another well-known advantage is their ability to handle both large displacements and large deformations. Mass-spring systems have some drawbacks. Since the model is tuned through its spring constants, good values for these constants are not always easy to derive from measured material properties. Furthermore, it is difficult to express certain constraints (like incompressibility and anisotropy) in a natural way. Another problem occurs when spring constants are large. Such large constants are used to model nearly rigid objects, or model non-penetration between deformable objects. This problem is referred as *stifness*. Stiff systems are problematic because of their poor stability, which requires small time steps for numerical integration resulting in slow simulation [9].

2.2. Finite Element

Whereas mass-spring models start with a discrete object model, more accurate physical models consider deformable objects as a continuum: solid body with mass and energies distributed throughout. Models can be discrete or continuous but the method used for solving is discrete. Finite element method is used to find an approximation for a continuous function that satisfies some equilibrium expression. In FEM, the continuum (object) is divided into elements joined at discrete node points. A function that solves the equilibrium equation is found for each element.

FEM has been widely used in soft tissues modeling. Debunne et al. used a space and time adaptive level of detail, in combination with a large displacement strain tensor formulation [7]. To solve the system, explicit FEM was used where each element is solved independently through a local approximation, which reduces computational time. Hirota et al. used FEM in simulation of mechanical contact between nonlinearly elastic objects [10]. The mechanical system used as a case study was the human leg, more precisely, the Visible Human right knee joint and some of its surrounding bones, muscles, tendons and skin. The approach relied on a novel penalty finite element formulation based on the concept of material depth to compute skin, tendons and muscles deformation. By linearly interpolating pre-computed material depths at node points of the finite element mesh, contact forces can be analytically integrated over contacting regions without raising computational cost. The algorithm was implemented as a part of an implicit finite element program for dynamic, quasi-static and static analysis of nonlinear viscoelastic solids. High nonlinearity and anisotropy typically observed for biological materials were also supported. To achieve real-time deformation, reducing computing time is necessary. Bro-Nielsen and Cotin studied this problem by using a condensation technique [4]. With this method, the computation time required for the deformation of a volumetric model can be reduced to the computation time of a model only involving the surface nodes of the mesh.

Finite element methods provide a more realistic simulation than mass-spring methods but are less computationally efficient. In addition, the linear elastic theory used to derive the potential energy equation assumes small deformation of the object, which is true for materials such as metal. However, for soft biological material, objects dimensions can deform in large proportions so that the small deformation assumption no longer holds. Because of this change, the amount of computation required at each time is greatly increased.

3. Deformable Model

Our approach to model soft tissues is inspired from the work of Jansson et al. [11]. Their work exploits a generalized mass-spring model – which they call molecular model – where mass points are, in fact, spherical mass regions called molecules. Elastic forces are then established between molecules by a spring-like connection.

Our contribution to this model is in the integration of properties of real biological materials to define the stiffness of its spring-like connections. We tested several approaches and selected the one that we can generalize for arbitrary distributions of masses and springs. The rheological standard to define the elasticity of a material is Young's modulus. Young's modulus is a property of a material, not of an object. So, it is independent of the object's shape. However, when one discretizes an object by a set of springs, the stiffness k of every spring must be proportional to the fraction of the volume of the object it represents. It means that if a cube of side l_0 is compressed by a force F, it should shorten in the direction of the force, of the same elongation variation Δl both if it is represented by only one spring and if it is discretized by n springs. Equation 3 establishes the Young's modulus E from the knowledge of the elongation variation Δl, an applied force F, the length of the object in rest conditions l_0, and the cross-sectional area of the object A. Applying Eq.3 iteratively in the simulation loop we can minimize the difference between the obtained and the aimed E increasing or reducing the value of k's accordingly. See more details in [18].

The Force Model. The model is described by two sets of elements: E, a set of spherical massive elements (molecules), and C, a set of connections between the elements in E (Eq. 1).

$$E=\{e_1,e_2,\cdots e_n\};\ C=\{C_{e_1},C_{e_2},\cdots C_{e_n}\};\qquad C_{e_i}=\{c_1,c_2,\cdots c_m\} \tag{1}$$

The model's behavior is determined by the forces produced on each element of E by each connection of C and some external forces.

$$\vec{F}_e=\vec{F}_G+\vec{F}_L+\vec{F}_C+\vec{F}_{collisions} \tag{2}$$

where

$$\begin{cases} \vec{F}_G=m_e\vec{g} & (3)\\ \vec{F}_L=-\Pi r_e^{\,2}\rho\left|\vec{V}_e\right|^2\dfrac{\vec{V}_e}{\left|\vec{V}_e\right|} & (4)\\ \vec{F}_C=\vec{F}_b+\vec{F}_d+\vec{F}_f & (5)\end{cases}$$

F_G: gravity (m_e is the mass of e and g is the gravity acceleration);
F_L: ambient viscous friction (r is the radius, *?* is the medium density and V is the velocity);
F_C: connection forces, see Eq. 6.

$$\vec{F}_C=\vec{F}_b+\vec{F}_d+\vec{F}_f \tag{6}$$

where

$$\begin{cases} \vec{F}_b=\sum_{i=0}^{|C_e|}-k_c\left(\left|\vec{P}_e-\vec{P}_p\right|-l_c\right)\dfrac{\vec{P}_e-\vec{P}_p}{\left|\vec{P}_e-\vec{P}_p\right|} & (7)\\ \vec{F}_d=\sum_{i=0}^{C_e}-b_c\left(\vec{V}_{\parallel}\right) & (8)\\ \vec{V}_{\parallel}=\dfrac{\left(\vec{V}_e-\vec{V}_p\right)\cdot\left(\vec{P}_e-\vec{P}_p\right)}{\left|\vec{P}_e-\vec{P}_p\right|^2}\left(\vec{P}_e-\vec{P}_p\right) & (9)\\ \vec{F}_f=\sum_{i=0}^{C_e}-\left|\mu_e\vec{F}_N\right|\dfrac{\vec{V}_{\perp}}{\left|\vec{V}_{\perp}\right|} & (10)\\ \vec{F}_N=\vec{F}_b+\vec{F}_d & (11)\\ \vec{V}_{\perp}=\left(\vec{V}_e-\vec{V}_p\right)-\vec{V}_{\parallel} & (12)\end{cases}$$

F_b: elasticity (k_c is the spring Hooke's constant, l_c is the spring elongation, and P_e and P_p are the positions of the elements involved with connection c);
F_d: internal damping (b_c is the damping coefficient, P and V are respectively the positions and velocities of the elements involved with connection c);
F_f: sliding friction (μ_e is the friction constant for the element and F_N is the force normal to friction direction).

$$E=\frac{F\cdot l_0}{\Delta l\cdot A} \tag{3}$$

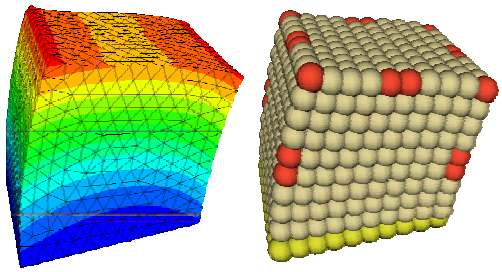

Figure 2. Comparison of results obtained with our deformable model (right) to results obtained with FEM (left) for the same setup.

To approach a validation for the model, we arranged a test setup to compare our results with results obtained by a Finite Elements static analysis. Two identical cubes have been created, one by colleagues from IMES-ETHZ (Institute of Mechanical Systems, Swiss Federal Institute of Technology Zürich) on their own FEM software, and the other using our implementation of the deformable model described above. The same Young's modulus was

used on the two objects, the same constant forces were applied onto them, and the results were compared. Visual results for a shear force applied on the upper face are shown in Figure 2. Besides the visual results that look similar, we also compared the displacement of key points tracked on both objects. These points represented on figure 2 by red spheres underwent the same displacements.

4. Anatomy-Based Kinematical Model

A kinematical model represents the human body articulated system as a tree where joints correspond to the nodes of the tree. Organs like bones and cartilage caps are instantiated into this node to give anatomical appearance to a human body part, (Figures 3). Any generic joint is able to describe any kind of relative motion between two or more adjacent segments of the body. Such motion can be given by: a) a rotation around one axis; b) a composed rotation around two or three axis; c) a translation in one to three Cartesian directions; d) rotations associated to translations; and e) an axis sliding on a parametric curve during rotation.

Figure 3. Sliding axis of a Joint. The rotation

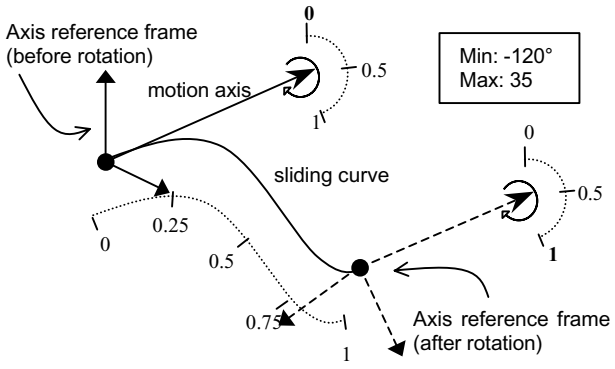

angle and the position on the curve are normalized within the range of motion and are defined by the same input parameter.

One particularity of our model – (e) above – is an approach to solve the problem of a joint center or axis that presents a displacement during motion. As the sliding axis move along a curved path, we chose to represent it by a standard parametric curve in 3D space. To be sure that the axis will slide on the curve, every time the angular parameter (normalized within the range of motion) of an axis changes, the same parameter is mapped in the curve equations to determine its respective point on it. The example in Figure 4 shows an axis angle and its reference frame position evolving according to the variation of the normalized angular parameter. More details can be found in [17].

5. Color Mapping

Color mapping is a common scientific visualization technique to display physical quantities on three-dimensional objects. Being effective and simple, it is widely used in CAD/CAM [12][8] and medical applications [16] for shape analysis. This technique consists in mapping scalar data to colors, and displaying the colors on the computer system. The scalar mapping is implemented by indexing into a color lookup table where scalars serve as indices.

Color mapping can also be performed by the use of transfer functions, which are expressions that map scalar values into color specifications. A lookup table is a discrete sampling of a transfer function and can be created from transfer functions by sampling them at discrete points [22].

Effective color mapping requires careful selection of color lookup tables and transfer functions. This selection requires sensitivity to the qualities of human perception and any special features in the data itself. Levkovitz studied the merits of color scales for medical images and introduced the notion of an optimal color scale [14].

In a previous work, we developed an automatic classification method for color maps [15]. Using different transfer functions (linear, S-curve, logarithmic, etc) and color domains, we generated 168 color tables that were projected onto a 2D layout, which makes exploration easy. This method is applied in this work to select appropriate color tables or transfer functions.

6. Application

Experimental results are illustrated in the case of a human hip joint. For instance, assessing stress and strain on the cartilage caps allows analyzing joint surface, which helps in diagnosis and surgical planning. An interactive test application was built. This application allows the user to visualize stress and strain on a model of human hip joint. With this application a user can change the point of view, choose to show or hide specific structures, use different color maps or use transparency to inspect internal parts that are usually masked.

3D boundary models of organs (meshes) are reconstructed from segmented MRI data [24]. The 3D meshes representing bones are considered rigid bodies and are used as is. Cartilage meshes have their volume discretized into a number of spherical regions representing the molecules of the deformation model (Figure 4).

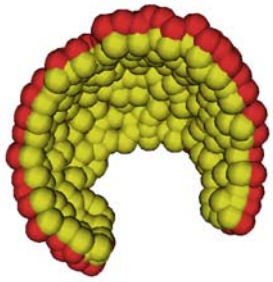

Figure 4. The cartilage cap of the acetabular cup discretized into a set of spherical regions.

The vertices on the surfaces of the cartilage caps are then linked to the neighborhood of underlying molecules with weights according to distances, and follow the model deformations. Surface molecules are used to generate contact avoidance forces. These forces, that are calculated using a penalty method [19], are consequently used by the deformation model to produce deformation. Motion is generated using the kinematical model (Figure 5). Finally, stress is calculated relating these forces with their area of actuation, and strain is calculated relating the original and current distances between molecules centers.

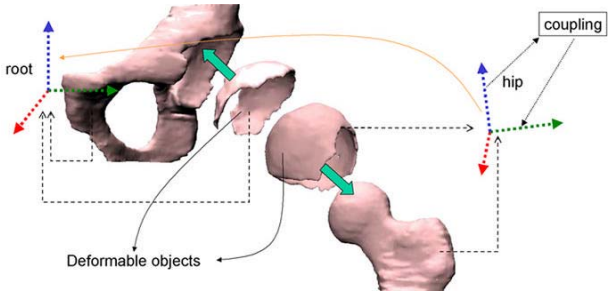

Figure 5. Kinematical hip. In this model the usual rotational axes are not constrained to rotate around a fixed point. The center of rotation can slide according to the angular position of the joint.

The last step is using color mapping for effective visualization of these values (Figures 6). Interactive visualization techniques allow free exploration of the simulation setup (Figure 7). All six images display the same posture but with different options: in the image (a) all surfaces are visible; in (b) acetabular parts are transparent to reveal a hidden surface of the femoral cartilage cap; in (c) the opposite, femoral parts are hidden and a user can inspect stress on the acetabular cartilage (virtual camera is displaced to see the interior); in (d), both cartilage caps are visible while bones are invisible; in (e) and (f) we have respectively the acetabular and femoral cartilage surfaces only. A simulation of evolving stress during motion is also presented on Figure 8.

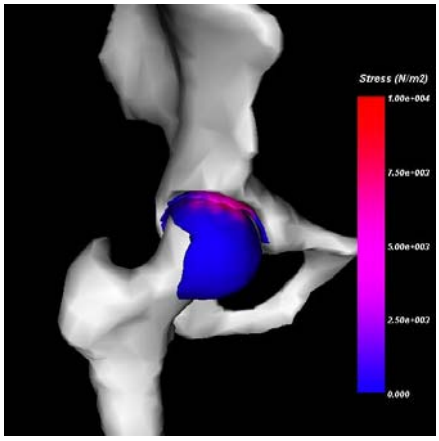

Figure 6. Stress distribution mapping on hip joint cartilage using a S-curve, blue-to-red transfer function.

7. Summary

In this paper, we have presented the combination of a deformable model for biological soft tissues with an anatomy-based kinematical model of human joints, which we used to simulate motion on the hip joint and evaluate stress and strain on cartilage surfaces.

The model demonstrated its ability to handle the stress-strain computation for two coupled surfaces with interactive user control. Associated to our palette of visualization tools, the user interaction can easily highlight regions subject to high stress, hence to pathologies.

At this moment, the deformation model is linear elastic and isotropic. We are working to improve it by adding viscous components and considering fibers orientation in the tissue. We aim at making it a viscoelastic, anisotropic and heterogeneous model, which is closer to the nature of the real biological tissues. It is crucial to support the envisaged medical applications. Future work also includes the evaluation of joint range of motion using the information given by stress distribution.

8. Acknowledgement

This work was supported by the Swiss National Science Foundation (SNF) in the framework of the National Center of Competence in Research for Computer Aided and Image Guided Medical Interventions (NCCR/CO-ME). We thank Lydia Yahia-Cherif from the MIRALab at University of Geneva for providing the 3-D models and Dr. Hassan Sadri, MD, from the Orthopedics

Department of the Fribourg Hospital for his support with the simulation of the hip joint.

References

[1] A. Aubel, and D. Thalmann, "Interactive Modeling of Human Musculature", *Computer Animation 2001*, Seoul, Korea, November 7-8, 2001.

[2] D. Baraff, and A. Witkin, "Large Steps in Cloth Simulation", *Proceedings of ACM SIGGRAPH'98*, ACM SIGGRAPH, 1998, pp. 43-54.

[3] D. Bourguignon, and M.-P. Cani, "Controlling Anisotropy in Mass-Spring Systems", *Computer Animation and Simulation 2000*, Interlaken (Switzerland), August 21-22, 2000, pp. 113-123.

[4] M. Bro-Nielsen, and S. Cotin, "Real-time Volumetric Deformable Models for Surgery Simulation using Finite Elements and Condensation", *Computer Graphics Forum (Eurographics'96)*, 15(3), 1996, pp. 57-66.

[5] J. Brown, S. Sorkin, C. Bruyns, J.-C. Latombe, K. Montgomery, and M. Stephanides, "Real-Time Simulation of Deformable Objects: Tools and Application", *In Computer Animation 2001*, Seoul, Korea, November 7-8, 2001.

[6] B. Z. A. Cohen, D. M. McCarthy, S. D. Kwark, P. Legrand, F. Fogarasi, E. J. Ciaccio, and G. A. Ateshian. "Knee Cartilage Topography, Thickness, and Contact Areas from MRI: in-vitro Calibration and in-vivo Measurements", *Osteoerthritis and Cartilage,* 7, OsteoArthritis Research Society International, 1999, pp. 95-109.

[7] G. Debunne, M. Desbrun, M.-P. Cani, and A. H. Barr, "Dynamic Real-Time Deformations Using Space and Time Adaptive Sampling", *Proceedings of SIGGRAPH 2001*, *Computer Graphics Proceedings,* ACM SIGGRPAH, August 2001, pp. 31-36.

[8] R. S. Gallagher and J. C. Nagtegaal, "An Efficient 3-D Visualization Technique for Finite Element Models and Other Coarse Volumes", *Proceedings of SIGGRAPH '89*, ACM SIGGRAPH, Boston, USA, July 31-August 4, 1989, pp. 185-193.

[9] S. F. Gibson, and B. Mirtich, "A Survey of Deformable Modeling in Computer Graphics", *Technical Report No. TR-97-19*, Mitsubishi Electric Research Lab., Cambridge, USA, November 1997.

[10] G. Hirota, S. Fisher, C. Lee, A. State, and H. Fuchs, "An Implicit Finite Element Method for Elastic Solids in Contact", *Computer Animation 2001*, Seoul (Korea), 2001.

[11] J. Jansson, and J. S. M Vergeest, "A Discrete Mechanics Model for Deformable Bodies", *Computer-Aided Design*, Vol. 34 (12), Elsevier Science, Amsterdam, 2002, pp. 913-928.

[12] S. Kuschfeldt, T. Ertl, and M. Holzner, "Efficient Visualization of Physical and Structural Properties in Crash-Worthiness Simulations (Case Study)", *In Proceedings of IEEE Visualization '97*, IEEE Computer Society and ACM, Phoenix, USA, October 19-24, 1997, pp. 487-490.

[13] Y. Lee, and D. Terzopoulos and K. Waters, "Realistic Modeling for Facial Animation", *Proceedings of SIGGRAPH 95, Computer Graphics Proceedings, Annual Conference Series*, Los Angeles, USA, August 1995, pp. 55-62.

[14] H. Levkowitz, and G. T. Herman, "Color Scales for Image Data", *IEEE Computer Graphics & Applications*, 12 (1), IEEE Computer Society, USA, 1992, pp. 72-80.

[15] I. S. Lim, P. H. Ciechomski, S. Sarni, and D. Thalmann "Planar Arrangement of High-dimensional Biomedical Data Sets by Isomap Coordinates", Proceedings *of the 16th IEEE Symposium on Computer-Based Medical Systems (CBMS 2003)*, IEEE Computer Society, New York, USA, June 26-27, 2003, pp. 50-55.

[16] I. S. Lim, S. Sarni, and D. Thalmann, "Colored Visualization of Shape Differences between Bones", *Proceedings of the 16th IEEE Symposium on Computer-Based Medical Systems (CBMS 2003)*, IEEE Computer Society, New York, USA, June 26-27, 2003, pp. 273-278.

[17] A. Maciel, L.P. Nedel and C.M.D.S. Freitas, "Anatomy-Based Joint Models for Virtual Human Skeletons", *Proceedings of the Computer Animation 2002 Conference*, Geneva, IEEE Computer Society, pp. 220-224, 2002.

[18] A. Maciel, R. Boulic, and D. Thalmann, "Deformable Tissue Parameterized by Properties of Real Biological Tissue" *In. International Symposium on Surgery Simulation and Soft Tissue Modeling, 2003*, Editors Nicholas Ayache & Herve Delingette, Springer-Verlag, Juan-les-Pins, France, 2003, pp.76-89.

[19] J.C. Platt and A. H. Barr. "Constraint Methods for Flexible Models", In Computer Graphics (Proc. SIGGRAPH), Vol. 22, No. 4, ACM SIGGRAPH, August 1988, pp. 279-288.

[20] L. Porcher-Nedel, and D. Thalmann. "Real Time Muscle Deformations Using Mass-Spring Systems", *Computer Graphics International 1998*, Hannover (Germany), June 1998, pp. 156-165.

[21] A. Radetzky, A Nürnberger, M. Teistler, D.P. Pretschner, "Elastodynamic shape modeling in virtual medicine", *International Conference on Shape Modeling and Applications*, IEEE Computer Society Press, Piscataway, NJ, 1999, pp. 172-178.

[22] W. Schroeder, K. Martin, and B. Lorensen, *The Visualization Toolkit: An Object-Oriented Approach to 3-D Graphics (2nd Edition),* Prentice Hall, New Jersey, USA, 1997.

[23] D. Terzopoulos, and K. Waters, "Physically-Based Facial Modeling, Analysis, and Animation", *The Journal of*

Visualization and Computer Animation, Vol. 1, December 1990, pp. 73-80.

[24] L. Yahia-Cherif, B. Gilles, L. Moccozet, N. Magnenat-Thalmann, "Individualized Bone Modelling from MRI: Application to the Human Hip", *in CARS 2003, Proceeding of the 16th International Congress Computer Assisted Radiology and Surgery*, Elsevier, London, UK, 2003.

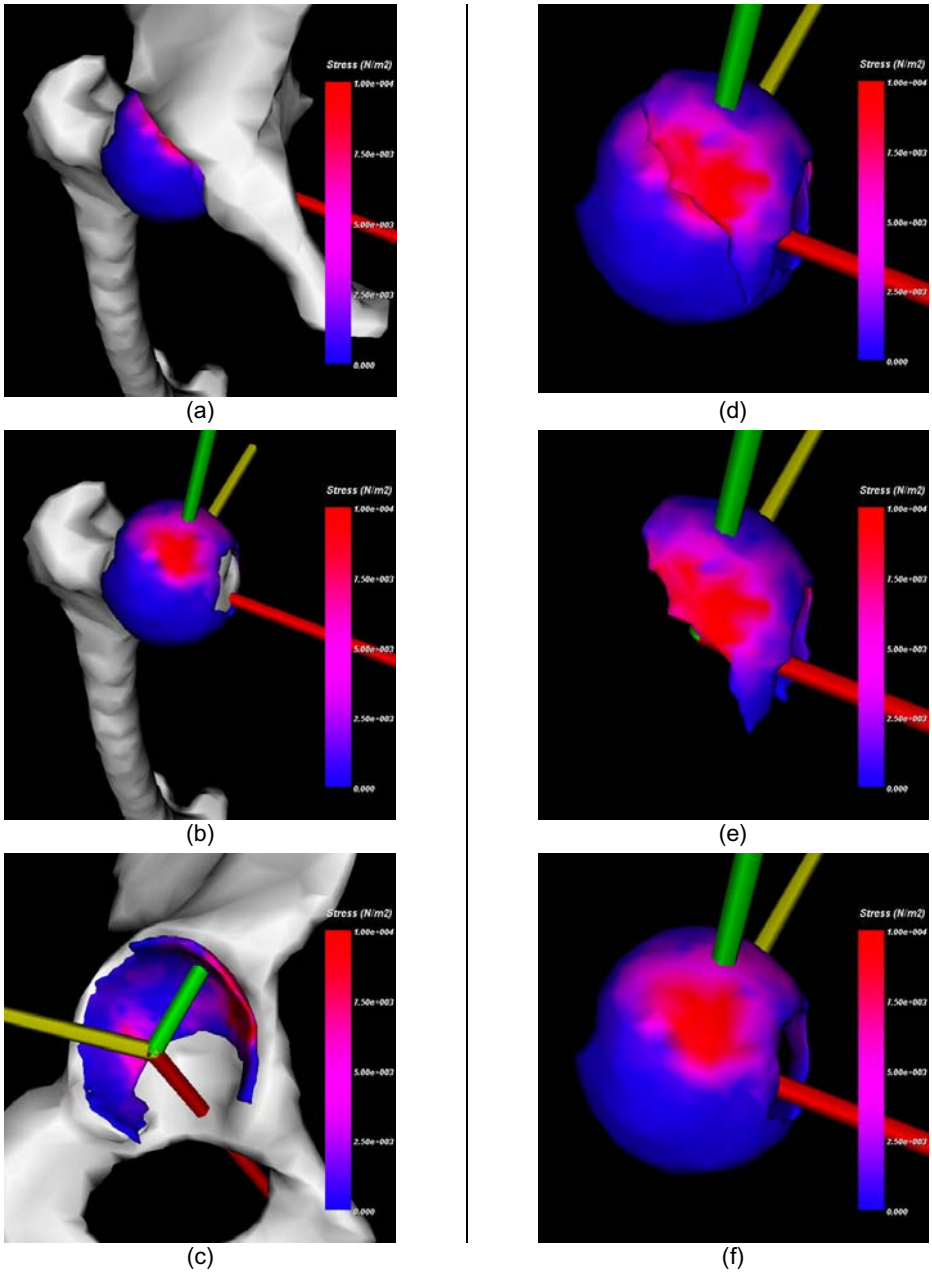

Figure 7. Different views of the problem. Interactive visualization techniques allow free exploration of the simulation setup. All six images display the same posture but with different options: in the image (a) all surfaces are visible; in (b) acetabular parts are transparent to reveal a hidden surface of the femoral cartilage cap; in (c) the opposite, femoral parts are hidden and a user can inspect stress on the acetabular cartilage (virtual camera is displaced to see the interior); in (d), both cartilage caps are visible while bones are invisible; in (e) and (f) we have respectively the acetabular and femoral cartilage surfaces only.

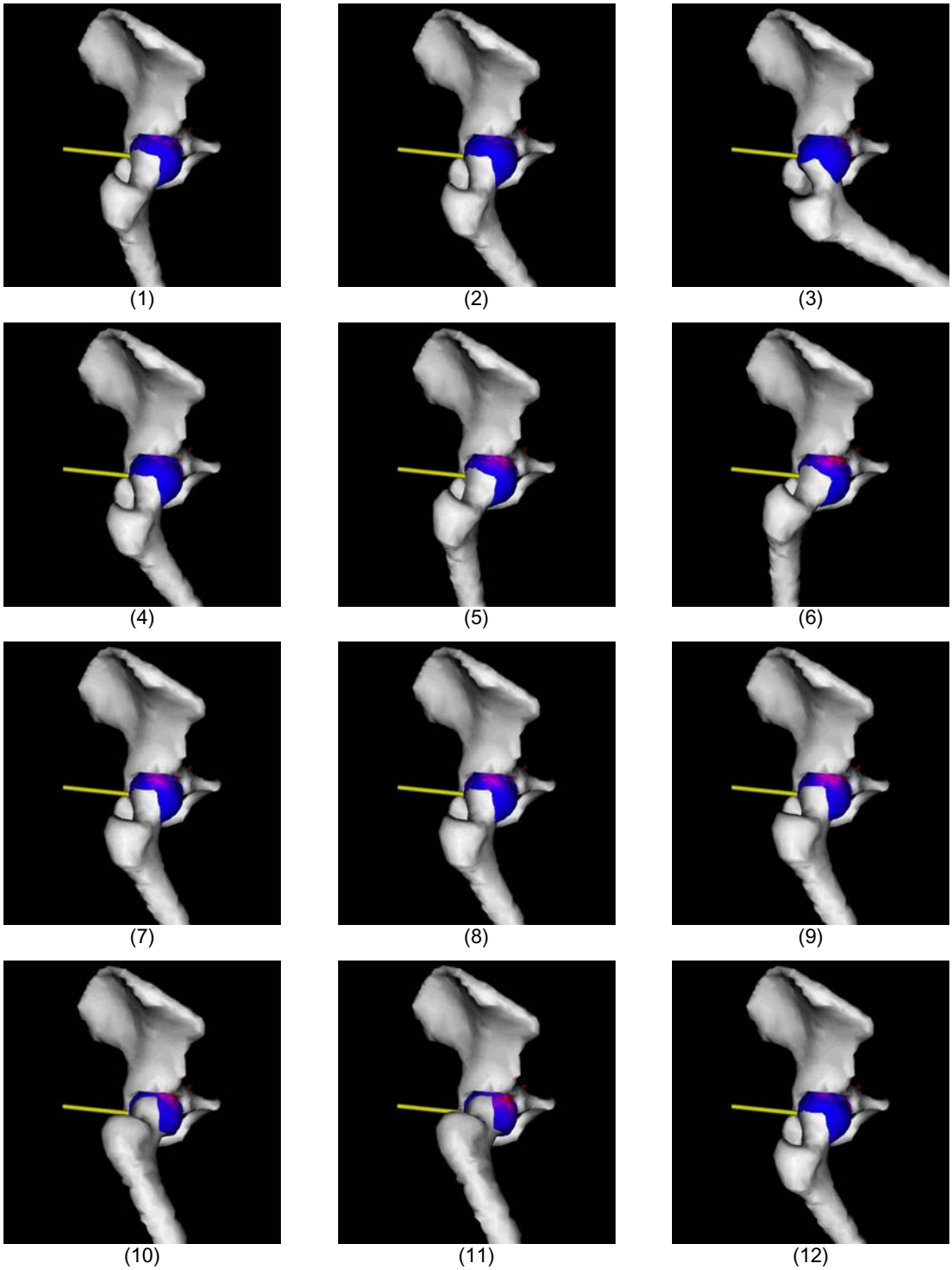

Figure 8. Simulated right hip joint evolving with stress mapped on cartilage surface. The frames 1 to 6 show a cycle of flexion-extension, and the frames from 7 to 12 show an abduction-adduction cycle. Note that stress is different for equivalent positions taken in forth or back motion because of dynamics.